TABLE V. HI and NT Titers of Sera Obtained From Animals Vaccinated With Whole Virion Vaccine Prepared From Akita 27 MG (+) or EgG (−)[a]

Vaccinated with	Antigens for assays					
	MG (+)		MG (−)		EgG (−)	
	HI	NT	HI	NT	HI	NT
MG (+)	13.2 ± 12.0	13.2 ± 4.6	13.2 ± 12.0	10.0 ± 0.0	17.4 ± 14.7	13.2 ± 4.6
EgG (−)	5.9 ± 4.1[b]	10.0 ± 0.0[c]	40.0 ± 7.6	20.0 ± 7.6[c]	47.6 ± 4.1	67.3 ± 4.1

[a]Titers were expressed as geometric mean ± SD of serum titers obtained from four or five animals receiving i.m. whole virion vaccine prepared from Akita 27 MG (+) or EgG (−). HI titers less than 10 and NT titers less than 20 were caluculated as titers of 5 and 10, respectively.
[b]Significantly different ($P < 0.005$) from the titer against EgG (−) as an antigen.
[c]Significantly different ($P < 0.01$) from the titer against EgG (−) as an antigen.

although this virus grew well in eggs. These contradictory results suggested that the absence of the glycosylation at 197 was necessary but not sufficient for egg-adaptation, and additional mutation(s) in other viral protein(s) might be required for optimal growth in eggs. Alymova et al. [1998] noticed that the NA activities differed among the viruses with different passage histories. An influenza B virus, isolated in egg showed higher NA activity than a virus isolated in mammalian cell line even though they originated from the same clinical specimen. Although not examined in this study, a difference in the NA activity might affect the release of mature viruses from infected cells. Comparison of deduced amino acid sequences of other viral proteins between the egg and the MDCK clones might reveal their involvement in the egg adaptation.

Both vaccine preparations examined in this study induced good protection in hamsters even against challenge by heterologous viruses (Table VI), although serum antibody response was apparently distinguishable between different vaccine preparations (Table V). Importantly to note was that Akita 27 MG (+) provided good protection, although HI and NI titers were apparently lower. It has been thought that the serum HI titer of ≥40 was required to protect from infection in humans. The discrepancy between the low HI titer and good protection level observed for MG (+) vaccinated group suggested that other viral component(s) might be involved in the protection. Such examples were seen in the case of influenza A virus for NA and M2 proteins [Kilbourne, 1976; Neirynck et al., 1999]. Another possibility that explains the discrepancy might be involvement of neutralization mechanism(s) other than direct inhibition of receptor binding measured by the HI test. Antibody-dependent complement components have been shown to display neutralizing activity against influenza viruses. Anti-HA antibody without detectable HI activity was shown to neutralize WS/33 influenza virus by activating the classical pathway of the complement system [Beebe et al., 1983]. Anti-HA monoclonal antibodies (MAbs) with low virus-neutralizing activity in vitro showed significant virus-neutralizing activity in vivo [Mozdzanowska et al., 1997]. Complement component C1q also enhanced the neutralizing activity of the anti-HA MAb in vitro [Feng et al., 2002]. MAb without HI activity was shown to neutralize virus infectivity, not by blocking receptor binding, but by interfering fusion activity of the HA molecule [Kida et al., 1985; Imai et al., 1998]. The observation that hamsters were protected from challenges in spite of the low HI titers against the challenge viruses in MG (+) vaccinated group, together with the instances above, suggested that serum HI antibody in vitro alone could not elucidate the protection efficacy in vivo.

TABLE VI. Efficacy of Whole Virion-Inactivated Vaccines Against Challenge With Different Clones of B/Akita/27/2001[a]

Vaccinated with	Challenged by	Number of infected animals (% protection)	Virus titer in lung of infected animals (log_{10} TCID/$_{50}$ml)
MG (+)	MG (+)	1/5 (80)	2.7
	MG (−)	0/5 (100)	–
	EgG (−)	1/5 (80)	4.7
EgG (−)	MG (+)	0/5 (100)	–
	MG (−)	1/4 (75)	≤1.7
	EgG (−)	0/5 (100)	–
Non-treat	MG (+)	5/5 (0)	4.98 ± 0.55[b]
	MG (−)	5/5 (0)	5.38 ± 0.30
	EgG (−)	5/5 (0)	5.38 ± 0.47

[a]Clone designation described in "Materials and Methods."
[b]Mean ± SD among five animals.

The lower immunogenicity of the MDCK derived clone observed in this study was in sharp contrast to the observation reported by Katz and Webster [1989] on the H3 influenza vaccine. Whether this is due to difference between influenza A and B viruses or a strain-specific phenomenon remains to be elucidated. A study of dose dependency using HA subunit vaccines made of the HA with or without the glycosylation 197 is necessary to evaluate the effect of glycosylation 197 on vaccine efficacy and immunogenicity precisely.

In conclusion, it was shown that antigenic properties of recent epidemic strains of influenza B viruses were influenced by the egg adaptation, suggesting that viruses isolated in mammalian cells are preferable as reference strains for antigenic surveillance of influenza virus. It is also important to monitor antigenic accordance between circulating strains and a vaccine strain to evaluate the suitability of a vaccine strain. Thus, the use of the mammalian culture derived strain as a vaccine strain is also preferable to avoid misleading evaluation by the egg-adaptation. The result also suggested that viral protein(s) other than HA appeared to be involved in the egg adaptation. Further study is necessary to understand the mechanisms of the egg adaptation of influenza B virus.

REFERENCES

Alymova IV, Kodihalli S, Govorkova EA, Fanget B, Gerdil C, Webster RG. 1998. Immunogenicity and protective efficacy in mice of influenza B virus vaccines grown in mammalian cells or embryonated chicken eggs. J Virol 72:4472–4477.

Beebe DP, Schreiber RD, Cooper NR. 1983. Neutralization of influenza virus by normal human sera: Mechanisms involving antibody and complement. J Immunol 130:1317–1322.

Berton MT, Naeve CW, Webster RG. 1984. Antigenic structure of the influenza B virus hemagglutinin: Nucleotide sequence analysis of antigenic variants selected with monoclonal antibodies. J Virol 52:919–927.

Feng JQ, Mozdzanowska K, Gerhard W. 2002. Complement component C1q enhances the biological activity of influenza virus hemagglutinin-specific antibodies depending on their fine antigen specificity and heavy-chain isotype. J Virol 76:1369–1378.

Gambaryan AS, Matrosovich MN. 1992. A solid-phase enzyme-linked assay for influenza virus receptor-binding activity. J Virol Methods 39:111–123.

Gambaryan AS, Robertson JS, Matrosovich MN. 1999. Effects of egg-adaptation on the receptor-binding properties of human influenza A and B viruses. Virology 258:232–239.

Gubareva LV, Wood JM, Meyer WJ, Katz JM, Robertson JS, Major D, Webster RG. 1994. Codominant mixtures of viruses in reference strains of influenza virus due to host cell variation. Virology 199:89–97.

Imai M, Sugimoto K, Okazaki K, Kida H. 1998. Fusion of influenza virus with the endosomal membrane is inhibited by monoclonal antibodies to defined epitopes on the hemagglutinin. Virus Res 53:129–139.

Katz JM, Webster RG. 1989. Efficacy of inactivated influenza A virus (H3N2) vaccines grown in mammalian cells or embryonated eggs. J Infect Dis 160:191–198.

Katz JM, Naeve CW, Webster RG. 1987. Host cell-mediated variation in H3N2 influenza viruses. Virology 156:386–395.

Kida H, Yoden S, Kuwabara M, Yanagawa R. 1985. Interference with a conformational change in the haemagglutinin molecule of influenza virus by antibodies as a possible neutralization mechanism. Vaccine 3:219–222.

Kilbourne ED. 1976. Comparative efficacy of neuraminidase-specific and conventional influenza virus vaccines in induction of antibody to neuraminidase in humans. J Infect Dis 134:384–394.

Matrosovich MN, Gambaryan AS, Tuzikov AB, Byramova NE, Mochalova LV, Golbraikh AA, Shenderovich MD, Finne J, Bovin NV. 1993. Probing of the receptor-binding sites of the H1 and H3 influenza A and influenza B virus hemagglutinins by synthetic and natural sialosides. Virology 196:111–121.

Meyer WJ, Wood JM, Major D, Robertson JS, Webster RG, Katz JM. 1993. Influence of host cell-mediated variation on the international surveillance of influenza A (H3N2) viruses. Virology 196:130–137.

Mozdzanowska K, Furchner M, Washko G, Mozdzanowski J, Gerhard W. 1997. A pulmonary influenza virus infection in SCID mice can be cured by treatment with hemagglutinin-specific antibodies that display very low virus-neutralizing activity in vitro. J Virol 71: 4347–4355.

Neirynck S, Deroo T, Saelens X, Vanlandschoot P, Jou WM, Fiers W. 1999. A universal influenza A vaccine based on the extracellular domain of the M2 protein. Nat Med 5:1157–1163.

Ohuchi M, Ohuchi R, Sakai T, Matsumoto A. 2002. Tight binding of influenza virus hemagglutinin to its receptor interferes with fusion pore dilation. J Virol 76:12405–12413.

Oxford JS, Corcoran T, Knott R, Bates J, Bartolomei O, Major D, Newman RW, Yates P, Robertson J, Webster RG, Schild GC. 1987. Serological studies with influenza A(H1N1) viruses cultivated in eggs or in a canine kidney cell line (MDCK). Bull World Health Organ 65:181–187.

Robertson JS, Naeve CW, Webster RG, Bootman JS, Newman R, Schild GC. 1985. Alterations in the hemagglutinin associated with adaptation of influenza B virus to growth in eggs. Virology 143:166–174.

Robertson JS, Bootman JS, Newman R, Oxford JS, Daniels RS, Webster RG, Schild GC. 1987. Structural changes in the haemagglutinin which accompany egg adaptation of an influenza A(H1N1) virus. Virology 160:31–37.

Robertson JS, Nicolson C, Bootman JS, Major D, Robertson EW, Wood JM. 1991. Sequence analysis of the haemagglutinin (HA) of influenza A (H1N1) viruses present in clinical material and comparison with the HA of laboratory-derived virus. J Gen Virol 72:2671–2677.

Saito T, Lim W, Suzuki T, Suzuki Y, Kida H, Nishimura SI, Tashiro M. 2001. Characterization of a human H9N2 influenza virus isolated in Hong Kong. Vaccine 20:125–133.

Schild GC, Oxford JS, de Jong JC, Webster RG. 1983. Evidence for host-cell selection of influenza virus antigenic variants. Nature 303:706–709.

Suzuki T, Jyono M, Tsukimoto M, Hamaoka A, Suzuki Y. 1995. Labeling of influenza virus with alkylamine-modified horseradish peroxidase. Anal Biochem 228:42–47.

Totani K, Kubota T, Kuroda T, Murata T, Hidari KI, Suzuki T, Suzuki Y, Kobayashi K, Ashida H, Yamamoto K, Usui T. 2003. Chemoenzymatic synthesis and application of glycopolymers containing multivalent sialyloligosaccharides with a poly (L-glutamic acid) backbone for inhibition of infection by influenza viruses. Glycobiology 13:315–326.

WHO. 1992. Standardization and improvement of influenza surveillance: Memorandum from a WHO/GEIG meeting. Bull World Health Organ 70:23–25.

WHO. 2001. Influenza in the world. 1 October 2000–30 September 2001. Wkly Epidemiol Rec 76:357–364.

WHO. 2003. Recommended composition of influenza virus vaccines for use in the 2003–2004 influenza season. Wkly Epidemiol Rec 78:58–62.

Wiley DC, Wilson IA, Skehel JJ. 1981. Structural identification of the antibody-binding sites of Hong Kong influenza haemagglutinin and their involvement in antigenic variation. Nature 289:373–378.

Wood JM, Oxford JS, Dunleavy U, Newman RW, Major D, Robertson JS. 1989. Influenza A (H1N1) vaccine efficacy in animal models is influenced by two amino acid substitutions in the hemagglutinin molecule. Virology 171:214–221.

Wright PF, Webster RG. 2001. Orthomyxoviruses. In: Knipe DM, Howley PM, editors. Fields virology, 4th edn. Philadelphia: Lipincott-Raven. pp 1533–1579.

International Immunology, Vol. 16, No. 10, pp. 1423–1430
doi:10.1093/intimm/dxh143 Advance Access publication 16 August 2004

A subcutaneously injected UV-inactivated SARS coronavirus vaccine elicits systemic humoral immunity in mice

Naomi Takasuka[1], Hideki Fujii[1], Yoshimasa Takahashi[1], Masataka Kasai[1], Shigeru Morikawa[2], Shigeyuki Itamura[4], Koji Ishii[3], Masahiro Sakaguchi[1], Kazuo Ohnishi[1], Masamichi Ohshima[1], Shu-ichi Hashimoto[1], Takato Odagiri[4], Masato Tashiro[4], Hiroshi Yoshikura[5], Toshitada Takemori[1] and **Yasuko Tsunetsugu-Yokota[1]**

[1]Department of Immunology, [2]First, [3]Second and [4]Third Departments of Virology, [5]National Institute of Infectious Diseases, Toyama 1-23-1, Shinjuku-ku, Tokyo 162-8640, Japan

Keywords: alum, cellular immunity, neutralizing antibody, parenteral administration, vaccination

Abstract

The recent emergence of severe acute respiratory syndrome (SARS) was caused by a novel coronavirus, SARS-CoV. It spread rapidly to many countries and developing a SARS vaccine is now urgently required. In order to study the immunogenicity of UV-inactivated purified SARS-CoV virion as a vaccine candidate, we subcutaneously immunized mice with UV-inactivated SARS-CoV with or without an adjuvant. We chose aluminum hydroxide gel (alum) as an adjuvant, because of its long safety history for human use. We observed that the UV-inactivated SARS-CoV virion elicited a high level of humoral immunity, resulting in the generation of long-term antibody secreting and memory B cells. With the addition of alum to the vaccine formula, serum IgG production was augmented and reached a level similar to that found in hyper-immunized mice, though it was still insufficient to elicit serum IgA antibodies. Notably, the SARS-CoV virion itself was able to induce long-term antibody production even without an adjuvant. Anti-SARS-CoV antibodies elicited in mice recognized both the spike and nucleocapsid proteins of the virus and were able to neutralize the virus. Furthermore, the UV-inactivated virion induced regional lymph node T-cell proliferation and significant levels of cytokine production (IL-2, IL-4, IL-5, IFN-γ and TNF-α) upon restimulation with inactivated SARS-CoV virion *in vitro*. Thus, a whole killed virion could serve as a candidate antigen for a SARS vaccine to elicit both humoral and cellular immunity.

Introduction

A new disease called severe acute respiratory syndrome (SARS) originated in China in late 2002 and spread rapidly to many countries. Upon this outbreak, a global collaboration network was coordinated by WHO. As a result of this unprecedented international effort, a novel type of coronavirus (SARS-CoV) was identified as the etiologic agent of SARS (1,2) in March 2003. The genomic sequence of SARS-CoV was completed and we now know that SARS-CoV has all the features and characteristics of other coronaviruses, but it is quite different from all previously known coronaviruses (groups I~III), representing a new group (group IV) (3,4). It is assumed that SARS-CoV is a mutant coronavirus transmitted from a wild animal that developed the ability to productively infect humans (3,5). The genome of SARS-CoV is a single-stranded plus-sense RNA ~30 kb in length and containing five major open reading frames that encode nonstructural replicase polyproteins and structural proteins: the spike (S), envelope (E), membrane (M) and nucleocapsid protein (N), in the same order and of approximately the same sizes as those of other coronaviruses (5).

The reason why SARS-CoV induces severe respiratory distress in some, but not all, infected individuals is still unclear. In patients with SARS and probable SARS cases, virus is detected in sputum, stool and plasma by RT-PCR (1,2). These patients developed serum antibodies against SARS-CoV and high antibody titers against N protein were maintained for more than 5 months after infection (6). Because of their generally poor pathogenicity and difficulty of propagation

Correspondence to: Y. Tsunetsugu-Yokota; E-mail: yyokota@nih.go.jp

Transmitting editor: K. Sugamura

Received 6 May 2004, *accepted* 15 July 2004

in vitro, there have been few studies regarding immunity to human coronaviruses OC43 and 229E. In the veterinary field, however, coronaviruses have been known for many years to cause a variety of lung, liver and gut diseases in animals. As we learned from these animal models, both humoral and cellular immune responses may contribute to protection against coronavirus diseases, including SARS [for review see (7)].

The clinical manifestation of SARS is hardly distinct from other common respiratory viral infections including influenza. Because an influenza epidemic may occur simultaneously with the re-emergence of SARS, it is urgently required that we develop effective SARS vaccines as well as sensitive diagnostic tests specific for SARS. Recently, the angiotensin-converting enzyme 2 (ACE2) was identified as a cellular receptor for SARS-CoV (8). The first step in viral infection is presumably the binding of S protein to its receptor, ACE2. In the murine MHV model, S proteins are known to contain important virus-neutralizing epitopes that elicit neutralizing antibodies in mice (9,10). Therefore, the S protein would be the first candidate coronavirus protein for induction of immunity. However, the S, M and N proteins are also known to contribute to generating the host immune response (11,12).

Following an established vaccine protocol is one of the best ways to shorten the time and cost of new vaccine development. Most of the currently available vaccines for humans are inactivated and applied cutaneously, except oral polio vaccine, and adjuvant usage is mostly limited to aluminum hydroxide gel (alum). In order to know the immunogenicity of inactivated SARS-CoV as a vaccine candidate, we immunized mice with UV-inactivated SARS-CoV either with or without alum. We report here the evaluation of humoral and cellular immunity elicited by UV-inactivated SARS-CoV administered subcutaneously.

Methods

Preparation of UV-inactivated purified SARS-CoV

SARS-CoV (HKU39849) was kindly supplied by Dr J.S.M. Peiris, Department of Microbiology, The University of Hong Kong. The virus was amplified in Vero E6 cells and purified by sucrose density gradient centrifugation. Concentrated virus was then exposed to UV light (4.75 J/cm^2) in order to inactivate the virus. We confirmed that the virus completely lost its infectivity by this method.

Immunization of mice

Female BALB/c mice were purchased from Nippon SLC Inc. (Shizuoka, Japan) and were housed under specific pathogen-free conditions. All experimental procedures were carried out under NIID-recommended guidelines. Mice were subcutaneously injected via their back or right and left hind leg footpads with 10 μg of UV-inactivated purified SARS-CoV with or without 2 mg of alum, and boosted by the same procedure 7 weeks after priming.

Detection of immunoglobulins in the serum samples

Blood was obtained from the tail vein and allowed to clot overnight at 4°C. Sera were then collected by centrifugation. For ELISA, microtiter plates (Dynatech, Chantily, VA) were coated overnight at 4°C with SARS-CoV-infected or mock-infected Vero E6 cell lysates, which had been treated with 1% NP40 followed by UV-inactivation. To detect S or N protein, the plates were coated with 1% NP40 lysates of chick embryo fibroblasts that had been infected with S or N protein-expressing DIs (attenuated vaccinia virus) (13). The plates were blocked with 1% OVA in PBS–Tween (0.05%) and then incubated with the sera serially diluted at 1:25–1:10^5 for 1 h at room temperature. Plates were incubated with either peroxidase-conjugated anti-mouse IgG (1:2000, Zymed, San Francisco, CA), IgM or IgA (1:2000, Southern Biotechnology, Birmingham, AL) antibody. For detection of IgG subclasses, either peroxidase-conjugated anti-mouse IgG_1, IgG_{2a}, IgG_{2b} (1:2000, Zymed) or IgG_3 (1:2000, Southern Biotechnology) was used. Plates were washed three times with PBS–Tween at each step. Antibodies were detected by *O*-phenylenediamine (Zymed), and the absorbance of each well was read at 490 nm using a model 680 microplate reader (Bio-Rad, Hercules, CA). As a standard for IgG detection, serum was obtained from a hyper-immunized mouse; the OD490nm value of 100 U/ml standard was ~3 in all assays. SARS-CoV-specific IgG titer was calculated as follows: SARS-specific IgG titer (U/ml) = (the unit value obtained at wells coated with virus-infected cell lysates) – (the unit value obtained at wells coated with non-infected cell lysates).

ELISPOT assay for antibody-secreting cells (ASCs)

Recombinant N protein (amino acids 1–49 and 340–390) of SARS-CoV (Biodesign, Saco, ME) was diluted to 10 μg/ml in PBS, and then added at 100 μl per well to plates supported by a nitrocellulose filter (Millipore, Bedford, MA). After overnight incubation at 4°C, the plates were washed with PBS three times and then blocked at 4°C overnight with 1% OVA in PBS–Tween (0.05%). After erythrocyte lysis, single cell suspensions from BMs were suspended in RPMI supplemented with 10% FCS, 5 × 10^{-5} M 2ME, 2 mM L-glutamine, 100 U/ml penicillin and 100 μg/ml streptomycin, and then applied to the plates at a concentration of 3 × 10^5 cells per well. After 24 h cultivation, the plates were recovered and stained with alkaline phosphatase-conjugated anti-mouse IgG_1 antibody (Southern Biotechnologies). Alkaline phosphatase activity was visualized using 3-amino-ethyl carbozole and napthol AS-MX phosphate/fast blue BB (Sigma). The frequency of plasma cells specific for N protein was determined from the N protein-coated plates after background on the uncoated plates was subtracted.

Coronavirus neutralizing assay

Serum was inactivated by incubation at 56°C for 30 min. The known tissue culture infectious dose (TCID) of SARS-CoV was incubated for 1 h in the presence or absence of serum antibodies serially diluted 5-fold, and then added to Vero E6 cell culture grown confluently in a 96-well microtiter plate. After 48 h, cells were fixed with 10% formaldehyde and stained with crystal violet to visualize the cytopathic effect induced by the virus (14). Neutralization antibody titers were expressed as the minimum dilution number of serum that inhibited the cytopathic effect.

Western blotting

Purified SARS-CoV virion (0.5 μg) was fractionated on SDS–PAGE under reduced conditions. Proteins were transferred to PVDF membrane (Genetics, Tokyo, Japan) and reacted with the diluted sera (1:1000) that had been obtained from mice inoculated with UV-irradiated SARS-CoV. After washing, the membrane was reacted with HRP-conjugated $F(ab')_2$ fragment anti-mouse IgG (H+L) (1:20 000 Jackson Immuno Research, West Grove, PA), followed by visualization of the bands on X-ray film (Kodak, Rochester, NY) using chemiluminescent regents (Amasham Biosciences, Piscataway, NJ).

Regional T cell response

Popliteal and inguinal lymph nodes and spleens were harvested from mice 1 week after the boost vaccination. After the preparation of a single cell suspension, T cells were purified by depletion of $B220^+$, $Gr1^+$, $CD11b^+$, IgD^+ and IgM^+ cells using a magnetic cell sort system (MACS: Miltenyi Biotec, Bergisch Gladbach, Germany). To prepare antigen-presenting cells (APC), normal BALB/c mouse splenocytes were depleted of $CD3^+$ T cells by MACS and irradiated at 2000 cGy.

Purified T cells taken from lymph nodes (1×10^5 cells/well) were cultured with irradiated APC (5×10^5 cells/well) in the presence or absence of UV-irradiated purified SARS-CoV virion (1 or 10 μg/ml). Four days after the cultivation, the level of cytokine concentration in the culture supernatant was measured by flow cytometry using a mouse Th1/Th2 cytokine cytometric bead array kit (Becton Dickinson, San Jose, CA). T-cell proliferation was monitored by the incorporation of [^{3}H]thymidine (18.5 kBq/well, ICN Biomedicals, Costa Mesa, CA) added 8 h prior to cell harvest. The cells were harvested on a 96-well microplate bonded with a GF/B filter (Packard Instruments, Meriden, CT). Incorporated radioactivity was counted by a microplate scintillation counter (Packard Instruments).

Results

Inoculation with UV-inactivated SARS-CoV results in an antigen-specific IgG_1 response, probably by generating long-term ASCs as well as memory cells

To examine the level of anti-SARS-CoV response in mice after inoculation with vaccine candidates, three mice in each group were subcutaneously inoculated with 10 μg of UV-inactivated purified SARS-CoV with (Virion/Alum) or without alum (Virion), or inoculated with alum alone (Alum) or left untreated (None) as a control (Fig. 1). One month after inoculation, vaccinated mice elicited the anti-SARS CoV IgG antibody in sera at high levels. As expected, the alum adjuvant enhanced the level of IgG antibody response, >10-fold higher than the level without adjuvant (Fig. 1C compared with B). When mice were boosted at 7 weeks, the level of IgG antibody in both groups of mice was further increased ~10-fold above the primary response (Fig. 1B and C). Notably, the level of serum antibodies induced by a single injection of virion, even in the absence of the alum adjuvant, was maintained at least more than 6 months (Fig. 1D). These results suggest that long-term ASCs can be established by a single shot of UV-inactivated virion administration.

Upon restimulation with antigen, memory B cells rapidly differentiate into ASCs and migrate into the bone marrow to establish a long-term ASC pool (15,16). To enumerate the number of plasma cells specific for SARS-CoV, we performed an ELISPOT assay using recombinant N proteins, amino acid numbers 1–49 (N1–49) and 340–390 (N340–390) as coating antigens. Consistent with the serum anti-SARS CoV IgG level, SARS-specific IgG_1 plasma cells were maintained in the bone marrow at day 10 after boost immunization with virion/alum

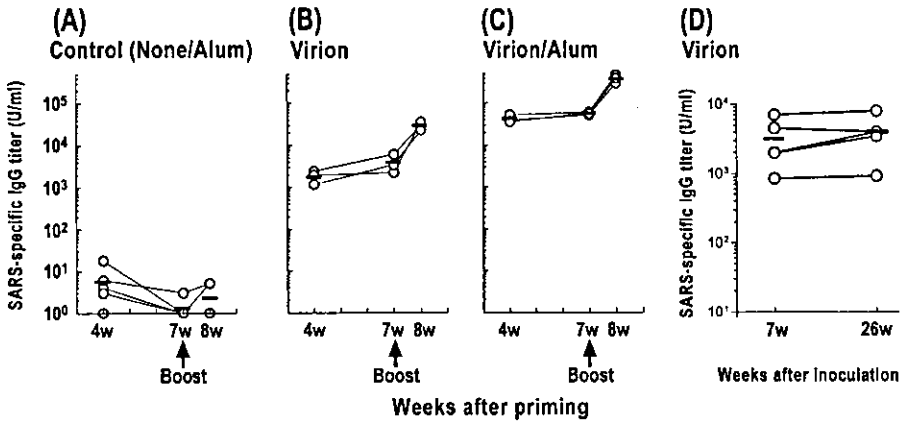

Fig. 1. The level of SARS-specific IgG in subcutaneously vaccinated mice. Mice were subcutaneously primed with 10 μg of UV-inactivated SARS-CoV virion (B), or virion with 2 mg of alum (C), or alum alone or none (A) and boosted with the same dose in their footpads at 7 weeks after priming. Serum was collected at the indicated time point and subjected to ELISA to detect SARS-specific IgG using SARS-CoV-infected Vero cell lysates as a coating antigen. Circles and bars represent the amount of IgG antibody in the serum of each mouse and the mean, respectively. The amount of IgG was arbitrarily calculated based on the concentration of hyper-immune sera. A representative result of two independent experiments is shown. (D) Mice were vaccinated with 10 μg of UV-inactivated SARS-CoV virion subcutaneously into their backs. Serum was collected from individual mice at the indicated time point and subjected to ELISA to detect SARS-specific IgG.

(Fig. 2). In contrast, the number of spots from control mice was below the detection limit (i.e. <1 ASC/9 × 10^5 cells).

UV-inactivated SARS-CoV induces IgG_1 antibody with neutralizing activity

We determined the subclass of serum anti-SARS-CoV IgG antibodies in the boosted mice using anti-mouse IgG_1, IgG_{2a}, IgG_{2b} or IgG_3 second antibody by ELISA (Fig. 3). Interestingly, the level of anti-SARS-CoV IgG_{2a} in mice immunized with virion/alum was comparable to that in mice immunized with virion alone, whereas the level of anti-SARS-CoV IgG_1 was higher in mice with virion/alum than the mice with virion alone. In contrast, the levels of IgG_{2b} and IgG_3 antibodies were fairly low in both groups. Therefore, our results indicated that vaccination with a combination of inactivated virion and alum induced a predominantly Th2-type immune response.

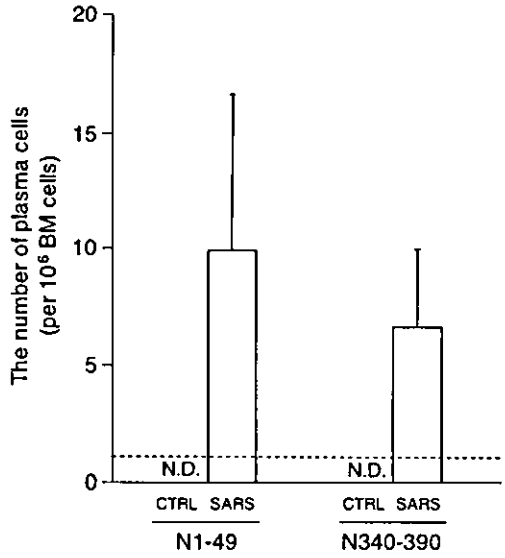

Fig. 2. The number of SARS-specific IgG_1 plasma cells in BM. Mice were primed and boosted by subcutaneous injection into their back with 10 μg of UV-inactivated SARS-CoV virion with 2 mg of alum (VA). BMs were collected at 10 days after boost and subjected to ELISPOT to detect SARS-specific IgG_1 plasma cells. Bars represent the number of plasma cells specific to N1–49 and N340–390 antigen in SARS-vaccinated and control mice, respectively. Data are means of triplicate cultures. The number of spots from control mice was below the detection limit (i.e. <1 ASC/9 × 10^5 cells: dashed line). A representative result of two independent experiments is shown. N.D.: not detected.

We also measured serum immunoglobulins other than IgG in the early and late phases of immunization. To avoid high IgG concentrations interfering with the detection of IgM and IgA antibodies, the serum IgG was absorbed with protein G-conjugated beads (>98%). The levels of anti-SARS-CoV IgM antibodies in the IgG-depleted sera, which were obtained 4 weeks after priming, were below our detection limit. Likewise, anti-SARS-CoV IgA antibody in the IgG-depleted sera, which were obtained 1 week after booster, was not detectable (data not shown).

Whether or not immune sera possess a neutralizing activity against SARS-CoV is a crucial aspect of vaccination. We estimated the neutralizing activity of sera obtained 1 week after boost inoculation (Table 1). We observed that neutralizing activity against SARS-CoV was detected at a high level in sera of mice inoculated with virion/alum or virion alone. Taken together, these results indicate that subcutaneous vaccination with UV-inactivated SARS-CoV virion is able to elicit a sufficient amount of IgG antibodies with neutralizing activity.

UV-inactivated SARS-CoV induces serum IgG antibody specific for S and N proteins

Using the immune sera of mice boosted with virion/alum 1 week before, we analyzed the specificity of serum IgG by western blot analysis (see Methods). As shown in Fig. 4(A), the robust signal detected at 50 kDa corresponds to the N protein of SARS-CoV, as predicted by its genome size (3,4). A band near 200 kDa appears to correspond to S protein, analogous with the S protein of other human coronaviruses, HCV-229E

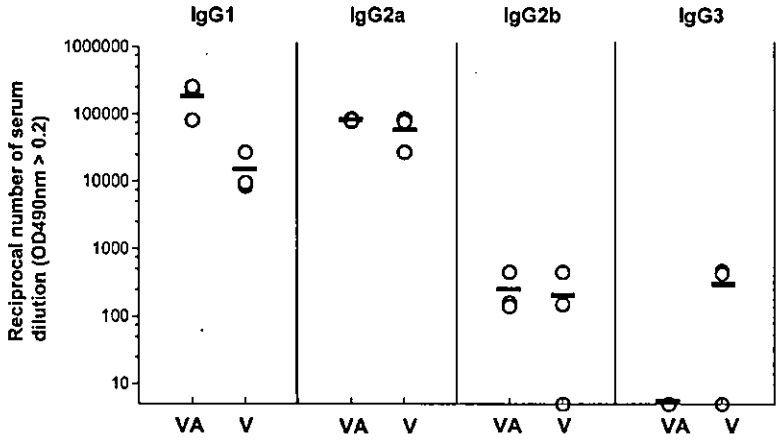

Fig. 3. IgG subclass of immunized serum. Mice were subcutaneously primed and boosted by injection in their footpads with 10 μg of UV-inactivated SARS-CoV virion (V), or virion with 2 mg of alum (VA). Serum was collected from individual mice at 1 week after boost and subjected to ELISA to detect SARS-specific IgG_1, IgG_{2a}, IgG_{2b} and IgG_3 titer. The Y value is the reciprocal serum dilution number where the OD490nm ≥ 0.2 in each ELISA. Circles and bars represent the titer for each mouse and the mean, respectively; results are representative of two separate experiments.

and HCV-OC43, which are known to be heavily glycosylated and detected at 186 kDa and 190 kDa, respectively (17). Our result is consistent with the data reported recently by Xiao *et al.* who expressed the full-length S glycoprotein of SARS-CoV Tor2 strain in 293 cells and showed that the protein ran ~180–200 kDa in SDS gels (18). The origins of the 120 kDa and the faint 37 kDa bands were unknown. However, similar bands were also detected on a fluorogram by using anti-N mAbs (Ohnishi, K., Sakaguchi, M., Takasuka, N. *et al.*, unpublished data), suggesting that it is related to N protein. The specificity of IgG in the immune sera was also determined by ELISA plates coated with lysates of cells infected with either S- or N-expressing recombinant vaccinia viruses (Fig. 4B). The results indicated that anti-S as well as anti-N protein IgG antibodies were elicited by virion/alum vaccination.

Table I. Neutralizing activity in serum after vaccination

		Reciprocal endpoint titer	
		Experiment 1	Experiment 2
None/alum		<5*	<5*
Virion	mouse 1	250	250
	2	1250	250
	3	1250	250
Virion/alum	1	250	1250
	2	1250	1250
	3	1250	1250

*All six mice examined did not have detectable neutralizing activity. Sera were obtained from mice 1 week after boost vaccination and subjected to SARS-CoV neutralizing activity assay as described in Methods. The titer is a reciprocal number of minimum serum dilution that inhibits the cytopathic effect.

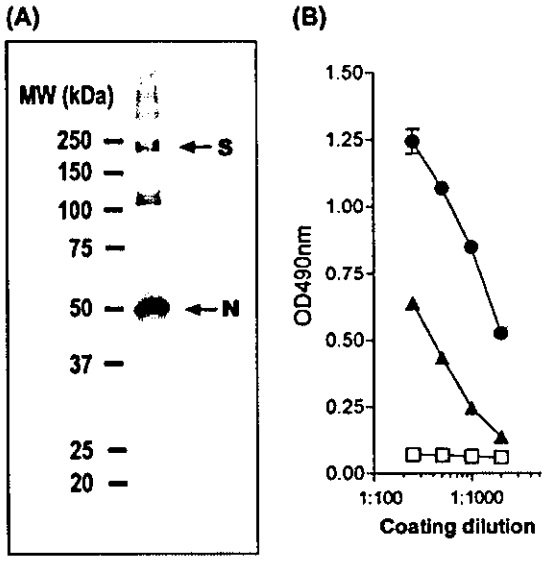

Fig. 4. Specificity of the serum antibodies. (A) Purified UV-inactivated SARS-CoV virion (0.5 μg) was fractionated by SDS-PAGE and subjected to western blotting. Diluted pooled sera (1:1000) from mice primed and boosted with virion/alum were exploited to detect virus proteins. Upper and lower arrows indicate the predicted band of S (spike protein) and N (nucleocapside protein) of SARS-CoV, respectively. The size of molecular weight markers (kDa) is shown on the left. (B) S protein- or N protein-specific ELISA. ELISA plates were coated at the indicated dilution with 1% NP40 lysates of chick embryo fibroblasts that had been infected with S protein-expressing vaccinia virus (circle), N protein-expressing vaccinia virus (triangle) or uninfected (mock; square). Diluted serum (1:1000) from mice prime and boost immunized with virion/alum, was exploited for detection of virus proteins.

UV-inactivated SARS-CoV whole virion induces T-cell response

To examine whether or not subcutaneously vaccinated mice gained an induced T-cell response against SARS-CoV, mice were immunized either with virion/alum, virion, or alum only via the footpad. T cells of these mice were enriched from the spleen and regional lymph nodes 1 week after a booster immunization and cultured with irradiated APCs in the presence or absence of UV-inactivated SARS-CoV virion at 1 or 10 μg/ml. As shown in Fig. 5(A), regional lymph node T cells proliferated *in vitro* in response to UV-inactivated virion in virion/alum-immunized mice and, to a lesser extent, in virion-immunized mice. Because mice inoculated with virion/alum showed a high basal level of proliferation of lymph node T cells in the absence of antigen, there is not much difference in the net proliferative response of these cells between the virion/alum group and the virion only group. On the other hand, in splenic T cells, a low level of proliferation was observed only in the virion/alum group of mice. The level of proliferation of these T cells, however, was virion-dose independent. Therefore, our results suggest that the subcutaneous injection of inactivated virion, even without alum, does induce T cell activation to some extent in the draining lymph node, a result which hardly occurs systemically.

We also measured the level of cytokine production in the supernatant of lymph node T cells stimulated with inactivated virion *in vitro* for 4 days. We found that the inactivated virion induced the production of all the cytokines (IL-2, IL-4, IL-5, IFN-γ and TNF-α) in T cells of virion/alum-immunized mice, in a dose-dependent manner (Fig. 5B). Likewise, T cells of virion-immunized mice produced low, yet significant, levels of these cytokines in a dose-dependent manner, except IL-5. In contrast, lymph node T cells from normal mice did not produce any cytokines at all in response to virion, suggesting that the virion itself does not possess innate stimulating activity as bacterial products [such as lipopolysaccharide (LPS) and purified protein derivative of mycobacterium tuberculosis (PPD)] do. Taken together, these results suggest that subcutaneous vaccination with UV-inactivated SARS-CoV is able to activate $CD4^+$ T cells in regional lymph nodes, where T cells produce several immunoregulatory cytokines, including IFN-γ.

Discussion

The present results demonstrated that even a single subcutaneous administration of UV-irradiated virion without alum adjuvant induced a high level of systemic anti-SARS-CoV antibody response in mice, probably followed by the generation of long-term antibody-secreting cells and memory cells in the bone marrow. Considering that polyvalent particulate

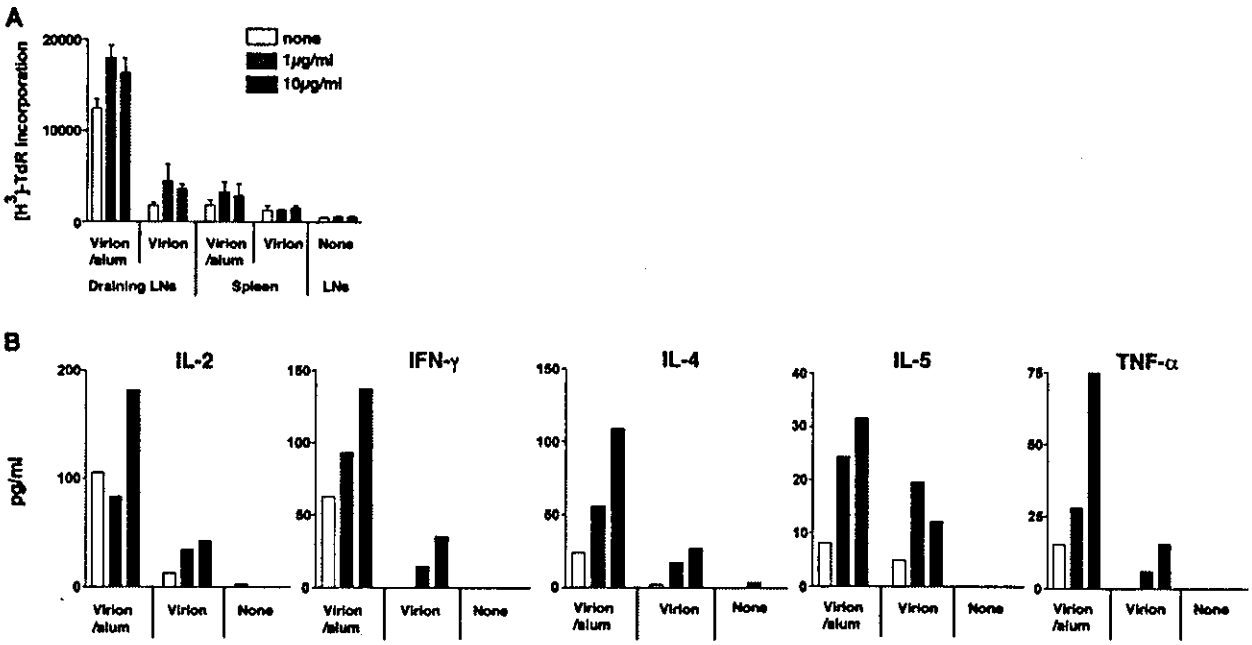

Fig. 5. *In vitro* responses of SARS-CoV-specific T cells taken from mice vaccinated with inactivated SARS-CoV. Mice were subcutaneously primed with 10 μg of UV-inactivated SARS-CoV virion, or virion with 2 mg of alum, or none, and then boosted with the same dose in their footpads at 7 weeks after priming. Draining lymph nodes and spleens were isolated at 1 week after boost and stimulated with T-cell depleted splenocytes that had been pulsed with the indicated concentration of UV-inactivated SARS-CoV virion. These cells were cultured for 2–4 days and [^{3}H]thymidine was added 8 h prior to the harvest. The peak response on day 4 after cultivation is shown in (A). (B) Culture supernatant was collected at day 2–4 post cultivation and the level of IL-2, IFN-γ, IL-4, IL-5 and TNF-α was determined by CBA kit. The maximum cytokine production at day 4 is shown. Results are representative of two separate experiments.

structures such as hepatitis B virus surface antigen-based, HIV-1 Gag-based and Ty virus-like particles have been shown to elicit humoral as well as cellular immune responses (19), these particulates probably have comparable dimensions and structures to the pathogens that are targeted for uptake by APCs to facilitate the induction of potent immune responses. The antibodies elicited in mice vaccinated by the current protocol with or without adjuvant recognized both the S and N proteins of SARS-CoV and were able to neutralize the infection of virus to Vero E6 cells. However, serum anti-SARS-CoV IgA antibody was not detectable, probably owing to the route of vaccination. In addition, the present vaccination protocol caused T cell response at the regional lymph nodes, although it did not allow for the induction of a sufficient cellular immune response systemically.

We show here the potentiality of subcutaneous injection of inactivated virion with alum, which is utilized for most of current human vaccinations. Alum has been used as an adjuvant for vaccines such as diphtheria, pertussis and tetanus, and these vaccines have a long safety record for human use (20). We observed that the addition of alum to the vaccine formula resulted in a large augmentation of serum IgG_1 production, but not IgG_{2a} production. The level of IgG_1 in alum-vaccinated mice reached a level similar to that found in hyper-immunized mice, which were subcutaneously injected with 5 μg of inactivated virion emulsified with a complete Freund adjuvant, followed by consecutive three-times intravenous boosters with 2 μg of virion. Alum is known to selectively stimulate an IgG_1 dominant, type 2 immune response [reviewed in (21)]. Activation of complement by alum could contribute to the type 2-biased immune response partly via an inhibition of IL-12 production. Interestingly, a quite recent report demonstrated that an alum-induced $Gr1^+$ myeloid cell population produced IL-4 and activated B-cells (22).

There are various diseases associated with animal coronavirus infection. The clinical manifestations of the disease and the correlates of protection with immunity have been studied extensively in these animal coronavirus infections [reviewed in (7)]. Although antibodies and T cells may play a role in exacerbating the pathology in some animal coronavirus infections (23,24), both humoral and cellular immune responses are known to contribute to protection against coronavirus infection. In murine hepatitis virus, a Group 2 coronavirus, the mortality of susceptible mice was partially prevented by the transfer of immune serum containing neutralizing antibody prior to challenge (25). Recently, Zhi-yong *et al.* reported in the murine acute infection model that the neutralizing antibody elicited by vaccination of DNA encoding S was protective, but cellular components of vaccinated mice were not required for the inhibition of viral replication (26). Because a twice parenteral administration of inactivated virion with alum induced a high level of antibodies that are able to neutralize SARS-CoV, this vaccination protocol may have a certain effect on the protection of humans from SARS-CoV infection.

We observed that two successive inoculations with inactivated virus at 7 week intervals generated SARS-CoV-specific

T cells. These cells were restimulated with the irradiated virus *in vitro*, but their response was low in terms of the level of proliferation and production of INF-γ and IL-2. However, irrespective of vaccination protocols with or without alum adjuvant, virus-primed T cells of vaccinated animals were capable of producing IL-4 at high levels upon *in vitro* stimulation, comparable to other reports for a variety of vaccination studies (27,28). This outlook seems compatible with the idea that the present vaccine protocol may tend to select T-cell subsets with Th2 phenotype. However, it remains to be elucidated whether such T cells may exhibit serological memory phenotype and persist in the immune system after vaccination as long as memory B cells, which may persist more than 180 days post vaccination. In addition, further analysis is needed to clarify whether T cell response is a crucial factor for long-term protection against SARS-CoV infections.

Efforts to develop a SARS-CoV vaccine have been carried out by many profitable or non-profitable organizations in various ways. For example, it has recently been reported that the combination of adenovirus vector expressing SARS-S, -M or -N protein elicited a neutralizing capacity in serum and N-specific T-cell response in rhesus macaques (29). However, it is still uncertain whether or not the immunity against only these components of SARS-CoV is sufficient for virus protection. SARS-CoV tends to cause replication errors, which may allow the virus to escape the host-immune response and result in a seasonal outbreak. From this point of view, it resembles influenza virus. In influenza virus, inactivated HA vaccine showed incomplete protection but had a certain efficacy and safety record for a long period of time. Indeed, this approach has been used in the veterinary field, such as with the bovine coronavirus (30) and canine coronavirus (31). These advantages make a whole killed virion a prime candidate for a SARS vaccine, even if it may not have the best protective ability.

Unfortunately, no information is available so far on the immune correlates of protection against human coronaviruses, including SARS-CoV. In consideration that SARS-CoV transmission occurs by direct contact with droplets or by the fecal oral route, mucosal secretary IgA in both the lower respiratory tract and digestive tract seem to be crucially important. Failure to induce IgA-type antibodies in a current systemic vaccination method should be improved. Notably, IgA antibodies were detectable in the sera and bronchoalveolar lavage fluid obtained from mice hyper-immunized with UV-irradiated virus (data not shown). Therefore, if a non-toxic and more potent adjuvant becomes available for human use, the subcutaneous injection of inactivated virion would become an effective vaccination method to reduce the number of susceptible people.

In the future, it will be necessary to determine whether or not the inactivated whole virion vaccine possesses protective ability against SARS-CoV infection by the use of adequate animal models. Furthermore, whether the alum addition augmented the protection and the effective period of SARS-CoV virion vaccination should be addressed, because currently used inactivated influenza virus whole virion vaccine is significantly effective without any adjuvant. Meanwhile, we also need to develop a potent adjuvant for induction of a much stronger mucosal immunity, in addition to evaluating available methods of virion inactivation.

Acknowledgements

We thank Ms R. Ishida, Ms Y. Kaburagi and Mr Y. Kimishima for their excellent technical help. This work was supported by a grant from the Ministry of Public Health and Labor of Japan.

Abbreviations

ACE2	angiotensin-converting enzyme 2
ASC	antibody-secreting cell
E	envelope
M	membrane
N	nucleocapsid protein
SARS	severe acute respiratory syndrome
SARS-CoV	SARS-associated coronavirus
S	spike protein

References

1 Drosten, C., Gunther, S., Preiser, W. *et al.* 2003. Identification of a novel coronavirus in patients with severe acute respiratory syndrome. *N. Engl. J. Med.* 348:1967.
2 Ksiazek, T. G., Erdman, D., Goldsmith, C. S. *et al.* 2003. A novel coronavirus associated with severe acute respiratory syndrome. *N. Engl. J. Med.* 348:1953.
3 Marra, M. A., Jones, S. J., Astell, C. R. *et al.* 2003. The genome sequence of the SARS-associated coronavirus. *Science* 300:1399.
4 Rota, P. A., Oberste, M. S., Monroe, S. S. *et al.* 2003. Characterization of a novel coronavirus associated with severe acute respiratory syndrome. *Science* 300:1394.
5 Holmes, K. V. and Enjuanes, L. 2003. Virology. The SARS coronavirus: a postgenomic era. *Science* 300:1377.
6 Liu, X., Shi, Y., Li, P., Li, L., Yi, Y., Ma, Q. and Cao, C. 2004. Profile of antibodies to the nucleocapsid protein of the severe acute respiratory syndrome (SARS)-associated coronavirus in probable SARS patients. *Clin. Diagn. Lab. Immunol.* 11:227.
7 De Groot, A. S. 2003. How the SARS vaccine effort can learn from HIV—speeding towards the future, learning from the past. *Vaccine* 21:4095.
8 Li, W., Moore, M. J., Vasilieva, N. *et al.* 2003. Angiotensin-converting enzyme 2 is a functional receptor for the SARS coronavirus. *Nature* 426:450.
9 Collins, R. A., Knobler, R. L., Powell, H. and Buchmeier, M. J. 1982. Monoclonal antibodies to murine hepatitis virus-4 (strain JHM) define the viral glycoprotein responsible for attachment and cell–cell fusion. *Virology* 119:358.
10 Fleming, J. O., Stohlman, S. A., Harmon, R. C., Lai, M. M., Frelinger, J. A. and Weiner, L. P.1983. Antigenic relationship of murine coronaviruses: analysis using monoclonal antibodies to JHM (MHV-4) virus. *Virology* 131:296.
11 Jackwood, M. W. and Hilt, D. A. 1995. Production and immunogenicity of multiple antigenic peptide (MAP) constructs derived from the S1 glycoprotein of infectious bronchitis virus (IBV). *Adv. Exp. Med. Biol.* 380:213.
12 Anton, I. M., Gonzalez, S., Bullido, M. J., Corsin, M., Risco, C., Langeveld, J. P. and Enjuanes, L. 1996. Cooperation between transmissible gastroenteritis coronavirus (TGEV) structural proteins in the *in vitro* induction of virus-specific antibodies. *Virus Res.* 46:111.
13 Ishii, K., Ueda, Y., Matsuo, K. *et al.* 2002. Structural analysis of vaccinia virus DIs strain: application as a new replication-deficient viral vector. *Virology* 302:433.
14 Storch, G. A. 2001. Diagnostic virology. In Knipe, D. M., Howley, P. M., ed., *Fields Virology*, 4th edn. Lippincott Williams & Wilkins, Philadelphia, PA. pp. 493–531.
15 Benner, R., Hijmans, W. and Haaijman, J. J. 1981. The bone marrow: the major source of serum immunoglobulins, but still a neglected site of antibody formation. *Clin. Exp. Immunol.* 46:1.
16 Slifka, M. K., Matloubian, M. and Ahmed, R. 1995. Bone marrow is a major site of long-term antibody production after acute viral infection. *J. Virol.* 69:1895.
17 Schmidt, O. W. and Kenny, G. E. 1982. Polypeptides and functions of antigens from human coronaviruses 229E and OC43. *Infect. Immun.* 35:515.

18 Xiao, X., Chakraborti, S., Dimitrov, A. S., Gramatikoff, K. and Dimitrov, D. S. 2003. The SARS-CoV S glycoprotein: expression and functional characterization. *Biochem. Biophys. Res. Commun.* 312:1159.
19 Singh, M. and O'Hagan, D. 1999. Advances in vaccine adjuvants. *Nat. Biotechnol.* 17:1075.
20 Clements, C. J. and Griffiths, E. 2002. The global impact of vaccines containing aluminium adjuvants. *Vaccine* 20 (Suppl. 3): S24.
21 HogenEsch, H. 2002. Mechanisms of stimulation of the immune response by aluminum adjuvants. *Vaccine* 20 (Suppl. 3): S34.
22 Jordan, M. B., Mills, D. M., Kappler, J., Marrack, P. and Cambier, J. C. 2004. Promotion of B cell immune responses via an alum-induced myeloid cell population. *Science* 304:1808.
23 Weiss, R. C. and Scott, F. W. 1981. Antibody-mediated enhancement of disease in feline infectious peritonitis: comparisons with dengue hemorrhagic fever. *Comp. Immunol. Microbiol. Infect. Dis.* 4:175.
24 Wu, G. F., Dandekar, A. A., Pewe, L. and Perlman, S. 2001. The role of CD4 and CD8 T cells in MHV-JHM-induced demyelination. *Adv. Exp. Med. Biol.* 494:341.
25 Pope, M., Chung, S. W., Mosmann, T., Leibowitz, J. L., Gorczynski, R. M. and Levy, G. A. 1996. Resistance of naive mice to murine hepatitis virus strain 3 requires development of a Th1, but not a Th2, response, whereas pre-existing antibody partially protects against primary infection. *J. Immunol.* 156:3342.
26 Yang, Z. Y., Kong, W. P., Huang, Y., Roberts, A., Murphy, B. R., Subbarao, K. and Nabel, G. J. 2004. A DNA vaccine induces SARS coronavirus neutralization and protective immunity in mice. *Nature* 428:561.
27 Mazumdar, T., Anam, K. and Ali N. 2004. A mixed Th1/Th2 response elicited by a liposomal formation of *Leishmania* vaccine instructs Th1 responses and resistance to *Leishmania donovani* in susceptible BALB/c mice. *Vaccine* 22:1162.
28 Nicollier-Jamot, B., Ogier, A., Piroth, L., Pothier, P. and Kohli, E. 2004. Recombinant virus-like particles of a norovirus (genogroup II strain) administered intranasally and orally with mucosal adjuvants LT and LT(R192G) in BALB/c mice induce specific humoral and cellular Th1/Th2-like immune responses. *Vaccine* 22:1079.
29 Gao, W., Tamin, A., Soloff, A., D'Aiuto, L., Nwanegbo, E., Robbins, P. D., Bellini, W. J., Barratt-Boyes, S. and Gambotto, A. 2003. Effects of a SARS-associated coronavirus vaccine in monkeys. *Lancet* 362:1895.
30 Takamura, K., Matsumoto, Y. and Shimizu, Y. 2002. Field study of bovine coronavirus vaccine enriched with hemagglutinating antigen for winter dysentery in dairy cows. *Can. J. Vet. Res.* 66:278.
31 Pratelli, A., Tinelli, A., Decaro, N., Cirone, F., Elia, G., Roperto, S., Tempesta, M. and Buonavoglia, C. 2003. Efficacy of an inactivated canine coronavirus vaccine in pups. *New Microbiol.* 26:151.

Microbiol. Immunol., 48(11), 905–909, 2004

Antibodies to Human-Related H3 Influenza A Virus in Baikal Seals (*Phoca sibirica*) and Ringed Seals (*Phoca hispida*) in Russia

Kazue Ohishi*[,1], Noriko Kishida[2], Al Ninomiya[3], Hiroshi Kida[2], Yoshitake Takada[4], Nobuyuki Miyazaki[4], Andrei N. Boltunov[5], and Tadashi Maruyama[1]

[1]*Research Program for Marine Biology and Ecology, Japan Agency for Marine-Earth Science and Technology (JAMSTEC), Yokosuka, Kanagawa 237–0061, Japan,* [2]*Department of Disease Control, Graduate School of Veterinary Medicine, Hokkaido University, Sapporo, Hokkaido 060–0818, Japan,* [3]*Laboratory of Influenza Viruses, Department of Virology 3, National Institute of Infectious Diseases, Musashimurayama, Tokyo 208–0011, Japan,* [4]*The University of Tokyo, Ocean Research Institute, Nakano-ku, Tokyo 164–8639, Japan, and* [5]*All-Russian Research Institute for Nature, Moscow, Russia*

Received June 21, 2004; in revised form, July 30, 2004. Accepted August 10, 2004

***Abstract*: Antibodies to influenza A virus were detected using enzyme-linked immunosorbent assay (ELISA) in the sera from two of seven Baikal seals (*Phoca sibrica*) and from five of six ringed seals (*Phoca hispida*) in Russia. In a hemagglutination-inhibition test using H1–H15 reference influenza A viruses, ELISA-positive sera from one Baikal seal and four ringed seals reacted to A/Aichi/2/68 (H3N2) and A/Bangkok/1/79 (H3N2) strains. One ringed seal serum sample reacted to A/seal/Massachusetts/1/80 (H7N7). The present results suggested that human-related H3 viruses were prevalent in Baikal seals and ringed seals inhabiting the central Russian Arctic.**

***Key words*: Influenza virus, Seal, Marine mammal**

Influenza A virus infects a variety of avian and mammalian species including humans and marine mammals such as seals and cetaceans (13, 19). Waterfowl are the primary host for all influenza A virus strains that have been introduced into mammals, including humans, as pandemic strains. It has been experimentally demonstrated that pigs serve as intermediate hosts to generate human pandemic strains (11). As interspecies transmission plays a crucial role in pandemic disease in new hosts, monitoring of the viral infections in animals, including wild animals, is important not only for the control of animal diseases but also for the prevention of human pandemics. Mass mortality associated with pneumonia occurred in harbor seals (*Phoca vitulina*) on the northeast coast of the U.S.A. in 1979–1980. A/seal/Massachusetts/1/80 (H7N7) influenza virus was isolated from dead animals during that outbreak (4, 12, 18). H4N5, H4N6, and H3N3 viruses were also isolated from dead seals in subsequent epizootics of pneumonia in the same location in 1982–1983 and 1991–1992 (1, 5). All of these seal viruses were of avian origin (1, 5, 8, 18). Serological investigations of the viral infection in marine mammals in the Barents Sea, Alaska, and Arctic Canada revealed that sporadic infections occurred in the animals (2, 3, 14, 17).

On the other hand, influenza B virus was isolated from a harbor seal, although influenza B virus had been believed to be a pathogen only for humans (16).

In a recent serological study of influenza virus infection in Caspian seals (*Phoca caspica*) that inhabit only the Caspian Sea, antibodies to human-related H3N2 virus were detected in 36% of the seals examined using enzyme-linked immunosorbent assay (ELISA) (15). Antibodies to influenza B virus were observed in 6% of the seals using ELISA (15). The purpose of this study is to examine the distribution of the viral infection and the viral subtypes in other seal species in Russia. Serological study was conducted in Baikal seals (*Phoca sibirica*) and ringed seals (*Phoca hispida*), which like Caspian seals belong to the genus *Phoca*.

Serum samples were collected under the Russian-Japanese Joint Research Program for Biological and

**Address correspondence to* Dr. Kazue Ohishi, Research Program for Marine Biology and Ecology, Japan Agency for Marine-Earth Science and Technology (JAMSTEC), 2–15 Natsushima, Yokosuka, Kanagawa 237–0061, Japan. Fax: +81–46–867–9525. E-mail: oishik@jamstec.go.jp

Abbreviations: ELISA, enzyme-linked immunosorbent assay; HI, hemagglutination-inhibition.

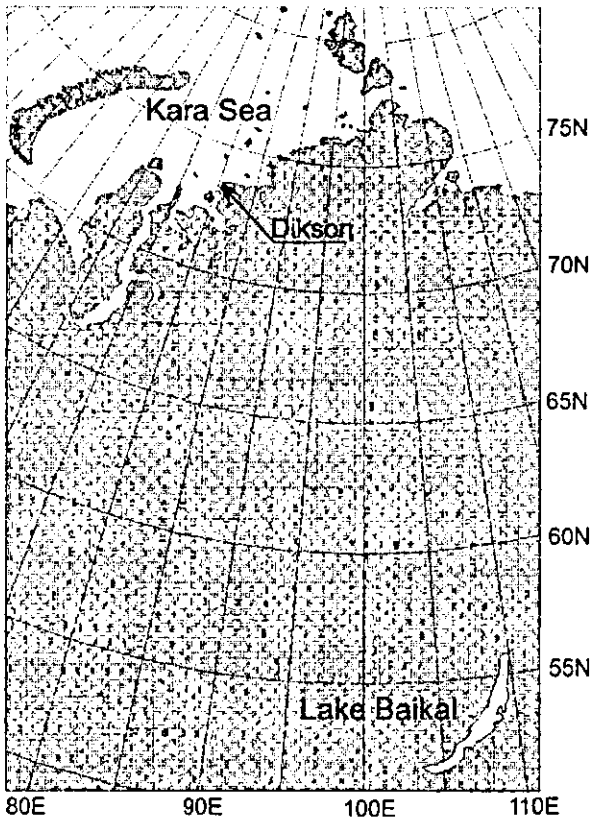

Fig.1. Map of the sampling areas. Serum samples from Baikal seals and ringed seals were collected in Lake Baikal in 1998, and in the southern part of the Kara Sea near Dikson settlement in 2002, respectively.

Environmental Studies with special permission from the local government. Sera were collected from seven (one female, six males) Baikal seals in Lake Baikal (53° 46–52′ N, 108° 23–31′ E), on May 21 and 22, 1998 (Fig. 1). All the Baikal seals were judged to be less than 1 year of age based on their body length (85–103 cm). Serum samples were collected from six (three females, three males) ringed seals in the southern part of the Kara Sea near Dikson settlement from May 2 to 22, 2002 (Fig. 1). The ringed seals were estimated to be 5.5–27.5 years of age based on an analysis of dental layers following Kasuya's method (7).

The following influenza viruses were from the repository of the Department of Disease Control, Hokkaido University, Graduate School of Veterinary Medicine: A/swine/Iowa/15/30 (H1N1), A/Singapore/1/57 (H2N2), A/Aichi/2/68 (H3N2), A/Bangkok/1/79 (H3N2), A/Philippines/2/82 (H3N2), A/Memphis/1/96 (H3N2), A/swine/Hong Kong/126/82 (H3N2), A/duck/Hokkaido/8/80 (H3N8), A/duck/Czechoslovakia/56 (H4N6), A/duck/Pennsylvania/10128/84 (H5N2), A/shearwater/Australia /1/72 (H6N5), A/seal/Massachusetts/1/80 (H7N7), A/turkey/Ontario/6118/67 (H8N4), A/chicken/Hong Kong/G24/98 (H9N2), A/chicken/Germany/N/49 (H10N7), A/duck/England/56 (H11N6), A/duck/Alberta/60/76 (H12N5), A/gull/Maryland/704/77 (H13N6), A/mallard/Astrakhan/263/82 (H14N5), A/duck/Australia/341/83 (H15N8), and B/Lee/40. Propagation and purification of the viruses were conducted according to previously described procedures (15). For analysis of the antibodies in seal sera, ELISA and the hemagglutination-inhibition (HI) test were conducted according to methods described previously (15).

Table 1. Antibodies to influenza A virus detected using ELISA in Baikal seals and ringed seals

Species	Positive rate[a]			Range of titer[b]
	Female	Male	Total	
Baikal seals	0/1	2/6	2/7	1,600–6,400
Ringed seals	3/3	2/3	5/6	800–12,800

[a] Percent positive (number positive/number tested). An absorbance value higher than 0.25 was regarded as positive according to the previous report (15).

[b] Titer was determined using the twofold serial dilution method.

Antibodies to influenza A virus were first screened with ELISA using seal sera diluted to 1:50. Purified A/Aichi/2/68 (H3N2) viruses were used as antigens. Antibodies were detected in two of the seven serum samples from Baikal seals and in five of six serum samples from ringed seals (Table 1). Serum samples judged as positive were further titrated using the twofold serial dilution method (Table 1). Antibodies to influenza B virus in the serum samples were examined with ELISA using purified B/Lee/40 as antigens, and no antibody was observed in any serum sample examined.

To determine the subtype of the hemagglutinin (HA) protein recognized by the serum antibodies, the HI test using the reference influenza A virus strains of each of the known HA subtypes (H1–H15) was carried out. ELISA-positive serum from one Baikal seal and sera from four ringed seals inhibited hemagglutination of the H3 virus strain (A/Aichi/2/68 (H3N2)) (Table 2a). One ringed seal serum responded weakly to the H7 virus strain (A/seal/Massachusetts/1/80) (H7N7) (Table 2a). To investigate the strain specificity of the antibodies detected in the above tests, the sera were further examined using the HI test for their reactivity to naturally occurring human H3N2 antigenic variants. The serum from one Baikal seal (B-35) reacted equally to both the A/Aichi/2/68 (H3N2) and A/Bangkok/1/79 (H3N2) strains (Table 2b). Serum samples from three ringed seals (R-2, R-5, and R-6) reacted only to the A/Aichi/2/68 (H3N2) strain, while one sample from a

Table 2. Hemagglutination-inhibition (HI) test of seal serum samples with influenza A viruses

a)

Influenza A virus strain (subtype)	Baikal seal	Ringed seal
A/swine/Iowa/15/30 (H1N1)	–	–
A/Singapore/1/57 (H2N2)	–	–
A/Aichi/2/68 (H3N2)	256	160, 320, 640, 1,280
A/duck/Czechoslovakia/56 (H4N6)	–	–
A/duck/Pennsylvania/10128/84 (H5N2)	–	–
A/shearwater/Australia/1/72 (H6N5)	–	–
A/seal/Massachusetts/1/80 (H7N7)	–	80
A/turkey/Ontario/6118/67 (H8N4)	–	–
A/chicken/Hong Kong/G24/98 (H9N2)	–	–
A/chicken/Germany/N/49 (H10N7)	–	–
A/duck/England/56 (H11N6)	–	–
A/duck/Alberta/60/76 (H12N5)	–	–
A/gull/Maryland/704/77 (H13N6)	–	–
A/mallard/Astrakhan/263/82 (H14N5)	–	–
A/duck/Australia/341/83 (H15N8)	–	–

b)

Virus strain bearing H3 HA	HI titer of seal serum samples				
	B-35	R-2	R-4	R-5	R-6
A/Aichi/2/68 (H3N2)	256	640	160	320	1,280
A/Victoria/3/75 (H3N2)	–	–	–	–	–
A/Bangkok/1/79 (H3N2)	256	–	80	–	–
A/Philippines/2/82 (H3N2)	–	–	–	–	–
A/Memphis/1/96 (H3N2)	–	–	–	–	–

c)

H3 influenza virus	HI titer of seal serum samples					
	R-1	R-2	R-3	R-4	R-5	R-6
A/Aichi/2/68 (H3N2)	–/160[a)]	640/640	–/–	160/160	320/320	640/640
A/sw/Hong Kong/126/82 (H3N2)	–/160	–/320	–/–	–/80	–/160	–/320
A/duck/Hokkaido/8/80 (H3N8)	–/–	–/–	–/–	–/–	–/–	–/–

The HI titer is expressed as the highest serum dilution that inhibited 4 units or 2 units of hemagglutination in Baikal or ringed seals, respectively. A titer higher than 80 was regarded as positive. – indicates a titer of less than 80. b, c) B-35, Baikal seal; R-1, -2, -3, -4, -5, -6, ringed seal. c) a) Titer in the conventional HI test/titer in the HI test with rosette antigens.

ringed seal (R-4) responded to the A/Aichi/2/68 (H3N2) and A/Bangkok/1/79 (H3N2) strains (Table 2b). These data suggested that infections with A/Aichi/2/68 (H3N2)- and A/Bangkok/1/79 (H3N2)-related H3 influenza A viruses were prevalent in Baikal seals and ringed seals in the central Russian Arctic, and that sporadic infection with H7 virus occurred in ringed seals.

A/swine/Hong Kong/126/82 (H3N2) and A/duck/Hokkaido/8/80 (H3N8) share similar antigenicity with A/Aichi/2/68 (H3N2) based on the analysis with H3 HA-specific monoclonal antibodies (10, 20). However, there are discrepancies between the antigenicity results in the HI test and ELISA with soluble antigens to these viruses (10). To examine the reactivity of the seal sera to the two viruses, the conventional HI test and the test with rosette antigens were conducted using all ringed seal samples. The sera did not inhibit the hemagglutination of the two viruses in the conventional HI test. However, four samples (R-2, -4, -5 and -6) inhibited the hemagglutination of A/swine/Hong Kong/126/82 (H3N2) rosette antigens at a lower titer than they inhibited that of A/Aichi/2/68 (H3N2) (Table 2c). One sample (R-1) which had been negative in conventional test using A/Aichi/2/68 (H3N2), showed positive in HI test with A/Aichi/2/68 (H3N2) and A/swine/Hong Kong/126/82 (H3N2) rossett antigens. These results showed that the seal sera specifically reacted to H3 virus related to A/Aichi/2/68 (H3N2).

In a previous report, we suggested that A/Bangkok/1/79 (H3N2)-related virus infected Caspian seals (15). That previous finding and the present results

together indicate that human-related H3N2 virus might be widely prevalent in seal populations inhabiting Lake Baikal, the Caspian Sea and the Arctic Sea in Russia. They might also indicate that H3N2 viruses are well-adapted to seal cells. Seals are terrestrial and aquatic habitants. They breed, reproduce, and nurse children on the land or ice, whereas they feed in waters. Seals have a chance to contact humans. They are often caught by hunters as valuable materials for fur production and as food for farmed minks in Lake Baikal and the Arctic Ocean. Recent expansion of human economic activity in Russia to the habitat of the seals might increase the possibility of transmission of the viruses from humans to seals. Specific receptors on target organs is a major factor in the host range restriction of influenza A viruses. A previous study showed the presence of *N*-acetylneuraminic acid-α2,3-galactose (NeuAcα2,3Gal) in seal lung tissues, which has high affinity with avian and equine viruses, but low affinity with human influenza A viruses (6). This discrepancy may indicate that seal cells may have another influenza virus receptor.

Estimation of age in the three species of seals indicated that the viruses were prevalent in Caspian seals, ringed seals, and Baikal seals at least until 1993, 1995, and 1997, respectively. The counterpart viruses had disappeared in humans because of rapid change in the virus in humans. This indicates that the viruses may have been maintained in seals in a similar manner as in ducks and pigs (9, 10). Because previous reports demonstrated that avian viruses can infect seals (1, 5, 8, 18), seals may play a role as "mixing vessel," similar to the role played by pigs (11). After the recent outbreaks of avian influenza in many Asian countries, monitoring of the virus in wild animals has been the focus of attention. Study of influenza virus infection including viral isolation in marine mammals, is important for understanding of ecology of the virus, as well as for the control of the pandemics in humans.

References

1) Callan, R.J., Early, G., Kida, H., and Hinshaw, V.S. 1995. The appearance of H3 influenza viruses in seals. J. Gen. Virol. **76**: 199–203.
2) Danner, G.R., McGregor, M.W., Zarnke, R.L., and Olsen, C.W. 1998. Serologic evidence of influenza virus infection in a ringed seal (*Phoca hispida*) from Alaska. Mar. Mammal Sci. **14**: 380–384.
3) De Boer, G.F., Back, W., and Osterhaus, A.D.M. 1990. An ELISA for the detection of antibodies against influenza A nucleoprotein in humans and various animals species. Arch. Virol. **115**: 47–61.
4) Geraci, J.R., Aubin, D.J.St., Barker, I.K., Webster, R.G., Hinshaw, V.S., Bean, W.J., Ruhnke, H.L., Prescott, J.H., Early, G., Baker, A.S., Madoff, S., and Schooley, R.T. 1982. Mass mortality of harbor seals: pneumonia associated with influenza A virus. Science **215**: 1129–1131.
5) Hinshaw, V.S., Bean, W.J., Webster, R.G., Rehg, J.E., Fiorelli, P., Early, G., Geraci, J.R., and Aubin, D.J.St. 1984. Are seals frequently infected with avian influenza viruses? J. Virol. **51**: 863–865.
6) Ito, T., Kawaoka, Y., Nomura, A., and Otsuki, K. 1999. Receptor specificity of influenza A viruses from sea mammals correlates with lung sialyloligosaccharides in these animals. J. Vet. Med. Sci. **61**: 955–958.
7) Kasuya, T. 1976. Reconsideration of life history parameters of the spotted and striped dolphins based on cemental layers. Sci. Rep. Whal. Res. Inst. **28**: 73–106.
8) Kida, H., Brown, L., and Webster, R.G. 1982. Biological activity of monoclonal antibodies to operationally defined antigenic regions on the hemagglutinin molecule of A/seal/Massachusetts/1/80 (H7N7) influenza virus. Virology **122**: 38–47.
9) Kida, H., Kawaoka, Y., Naeve, C.W., and Webster, R.G. 1987. Antigenic and genetic conservation of H3 influenza virus in wild ducks. Virology **159**: 109–119.
10) Kida, H., Shortridge, K.F., and Webster, R.G. 1988. Origin of the hemagglutinin gene of H3N2 influenza viruses from pigs in China. Virology **162**: 160–166.
11) Kida, H., Ito, T., Yasuda, J., Shimizu, Y., Itakura, C., Shortridge, K.F., Kawaoka, Y., and Webster, R.G. 1994. Potential for transmission of avian influenza viruses to pigs. J. Gen. Virol. **75**: 2183–2188.
12) Lang, G., Gagnon, A., and Geraci, J.R. 1981. Isolation of an influenza A virus from seals. Arch. Virol. **68**: 189–195.
13) Murphy, B.R., and Webster, R.G. 1996. Orthomyxoviruses, p. 1397–1445. *In* Fields, B.N., Knipe, D.M., and Howley, P.M. (eds), Fields virology, 3rd ed, Lippincott-Raven Publishers, Philadelphia.
14) Nielesen, O., Clavijo, A., and Boughen, J.A. 2001. Serologic evidence of influenza A infection in marine mammals of Arctic Canada. J. Wildl. Dis. **37**: 820–825.
15) Ohishi, K., Ninomiya, A., Kida, H., Park, C.-H., Maruyama, T., Arai, T., Katsumata, E., Tobayama, T., Boltunov, A.N., Khursakin, L.S., and Miyazaki, N. 2002. Serological evidence of transmission of human influenza A and B viruses to Caspian seals (*Phoca caspica*). Microbiol. Immunol. **46**: 639–644.
16) Osterhaus, A.D.M.E., Rimmelzwaan, G.F., Martina, B.E.E., Bestebroer, T.M., and Fouchier, R.A.M. 2000. Influenza B virus in seals. Science **288**: 1051–1053.
17) Steuen, S., Have, P., Osterhaus, D.M.E., Arnemo, J.M., and Moustgaard, A. 1994. Serological investigation of virus infections in harp seals (*Phoca groenlandica*) and hooded seals (*Cystophora cristata*). Vet. Rec. **134**: 502–503.
18) Webster, R.G., Hinshaw, V.S., Bean, W.J., Van Wyke, K.L., Geraci, J.R., Aubin, D.J.St., and Petursson, G. 1981. Characterization of an influenza A virus from seals. Virology **113**: 712–724.
19) Webster, R.G., Bean, W.J., Gorman, O.T., Chambers, T.M., and Kawaoka, Y. 1992. Evolution and ecology of influenza A viruses. Microbiol. Rev. **56**: 152–179.

20) Yasuda, J., Shortridge, K.F., Shimizu, Y., and Kida, H. 1991. Molecular evidence for a role of domestic ducks in the introduction of avian H3 influenza viruses to pigs in Southern China, where the A/Hong Kong/68 (H3N2) strain emerged. J. Gen. Virol. 72: 2007–2010.

Acta Neuropathol (2004) 108: 485–492
DOI 10.1007/s00401-004-0909-0

REGULAR PAPER

Takuya Iwasaki · Shigeyuki Itamura
Hidekazu Nishimura · Yuko Sato · Masato Tashiro
Tsutomu Hashikawa · Takeshi Kurata

Productive infection in the murine central nervous system with avian influenza virus A (H5N1) after intranasal inoculation

Received: 11 March 2004 / Revised: 11 June 2004 / Accepted: 11 June 2004 / Published online: 8 October 2004

Abstract The H5N1 type of influenza A virus isolated from human patients in 1997 has a characteristic hemagglutinin and was considered to be directly transmitted from birds. Although neuropathogenicity of this virus was not demonstrated in human autopsy cases, some experimental studies using mice have disclosed that this virus infects the central nervous system (CNS) after intranasal inoculation. In this study we focused on the topographical localization of virus-infected cells in the murine CNS after intranasal inoculation. We immunohistochemically examined virus-infected cells in mouse tissues using a rabbit antiserum recognizing the nucleoprotein of influenza A virus. The virus-infected cells appeared initially in the respiratory tract. Thereafter, the virus antigen-positive cells appeared in the olfactory system and the cranial nerve nuclei innervating the facial region. This suggests that this virus is principally transmitted from the nasal cavity to CNS through the cranial nerves. Neurons were frequently infected and glial and ependymal cells were also infected. Transneuronal transmission of the virus might play the important role of viral spread within the CNS.

Keywords Influenza virus · H5N1 · Nucleoprotein · Immunohistochemistry · Brain

T. Iwasaki (✉) · Y. Sato · T. Kurata
Department of Pathology,
National Institute of Infectious Diseases,
Toyama 1-23-1, Shinjuku-ku, 162-8640 Tokyo, Japan
E-mail: tiwasaki@net.nagasaki-u.ac.jp

S. Itamura · M. Tashiro
Department of Virology III,
National Institute of Infectious Diseases,
Toyama 1-23-1, Shinjuku-ku, 162-8640 Tokyo, Japan

T. Iwasaki
Division of Clinical Investigation,
Institute of Tropical Medicine, Nagasaki University,
Sakamoto 1-12-4, 852-8523 Nagasaki, Japan

H. Nishimura
Virus Reference Center, National Sendai Hospital,
Sendai, Japan

T. Hashikawa
Laboratory for Neural Architecture,
Brain Science Institute, Riken, Wako,
351-0198 Saitama, Japan

Introduction

Influenza A virus is divided into subtypes by the antigenic nature of its surface glycoproteins of hemagglutinin (HA) and neuraminidase (NA) inserted in the envelope [12]. HA protein is known to be responsible for binding and penetration of virions to host cells. Among HA subtypes, three have been demonstrated to infect human beings and to have caused four pandemics in 1918 (H1N1, Spanish), 1957 (H2N2, Asian), 1968 (H3N2, Hong Kong) and 1977 (H1N1, Russian) [23]. As rare incidences, H7N7 virus was occasionally isolated from conjunctiva in 1980 and 1996 [11, 22]. H5N1 virus was first isolated from 18 human patients in Hong Kong in 1997 (6 of them died) [3, 19] and was considered to be directly transmitted from chicken. Biologically, H5N1 virus strains isolated during this outbreak were classified into two subgroups (Groups 1 and 2) by pathogenicity in mice [4] and by the antigenic character of HA protein [1]. In addition, H5N1 strains were again isolated from human patients in 2003–2004 in Thailand and Vietnam during the outbreak of avian influenza in Cambodia, China, Japan, Korea, Laos, Thailand and Vietnam.

Influenza A virus is transmitted by aerosol, and infects the mucosal epithelium [23]. Influenza virus infection within the central nervous system (CNS) has not been well demonstrated in human cases. Virological and pathological studies on experimental intranasal inoculation of H1N1 viruses revealed that the influenza virus infection was localized only in the columnar or alveolar epithelium of the respiratory

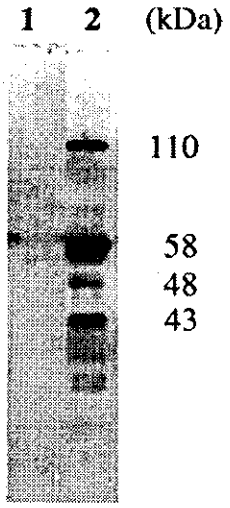

Fig. 1 Western blot analysis of the antibody recognizing the nucleoprotein of influenza A virus H5N1 used in the immunohistochemical study. *Lane 1*: MDCK cells without virus inoculation. *Lane 2*: MDCK cells inoculated with HK483 virus at 48 h p.i. (*p.i.* post inoculation)

tract [7, 9, 24, 25]. Only influenza viruses belonging to H5 and H7 subtypes have been demonstrated to infect CNS after intranasal inoculation in mice [4, 6, 13, 15, 16, 18]. In a previous report [15], we revealed that two Group 1 strains of H5N1 virus infected not only the respiratory tract, but also the CNS, adipose tissues, heart and liver after intranasal inoculation in mice. In this study, we further investigated the pathogenesis of CNS involvement in mice, using a Group 1 strain of H5N1 virus, by topographical analysis of virus-infected cells in the CNS.

Materials and methods

Mice and infection

All the experiments using a live H5N1 virus were performed in biosafety level 3 facilities under the recommended procedures. Animal care, breeding, virus inoculation, observation and sacrifice under deep anesthesia were performed in accordance with the guidelines of the Institutional Committees. Specific pathogen-free (SPF) 4- to 7-week-old outbred female mice (ddY) were obtained from the Japan SLC (Hamamatsu, Japan). Influenza A/Hong Kong/483/97 (HK483; H5N1) virus [4], isolated in the Government Virus Unit, the Queen Mary Hospital, Hong Kong, was prepared in Mardin-Darby canine kidney (MDCK) cells without any special step for mouse adaptation. We also used influenza A/Puerto Rico/8/34 (PR8; H1N1) virus prepared as described previously [20] as a control of classical influenza A virus. Mice were lightly anesthetized with intraperitoneal injection of sodium amobarbital (0.25 mg), and were inoculated intranasally with 2 µl or 20 µl of virus suspension containing 2×10^5 plaque forming unit (PFU) HK483 / mouse into the left or both nostrils.

Titration of virus

Viral titration of the brain and the lung tissues of infected mice was performed by a plaque assay method using MDCK cells. Tissue homogenate (10% w/v) was prepared in PBS (pH 7.2). The supernatant of homogenates after centrifugation at 3,000 rpm for 20 min was inoculated into the cells in the presence of 10 µg/ml acetylated trypsin (Sigma, St. Louis, MO).

Antibody and its characterization

For detection of HK483 virus, we used a polyclonal anti-influenza A nucleoprotein rabbit serum prepared by immunizing rabbits with the purified nucleoprotein of PR8 [20]. The specificity of this antibody to recognize the nucleoprotein of HK483 virus was confirmed by Western blot analysis. HK483 virus-infected and uninfected MDCK cells were lysed in Laemmli sample buffer with 2-mercaptoethanol, boiled for 10 min, and then subjected to 12% SDS-polyacrylamide gel electrophoresis. After electrophoretic transfer of proteins from gels to PVDF filters (Immobilon, Millipore, Bedford, MA), the filters were incubated in

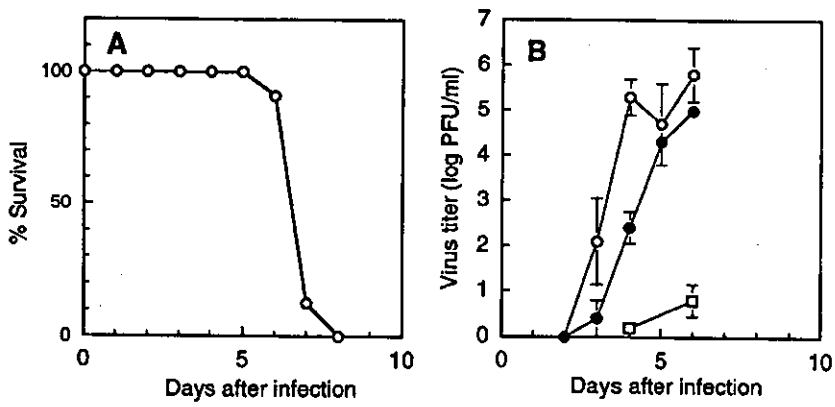

Fig. 2 Survival and virus titers of ddY mice after intranasal inoculation of HK483 virus. **A** Survival of mice after intranasal inoculation of 2 µl HK483 virus. **B** Mean ± SD of virus titers in the lungs (*open circles*), brain (*closed circles*) and blood (*open square*) of three mice on days 2, 3, 4, 5, and 6 p.i. Virus titers in the blood were examined on days 4 and 6

Table 1 Immunohistochemical detection of the virus-infected cells in mice infected by influenza A virus (H5N1, HK/483/1997). Values indicate the number of mice (*p.i.* post inoculation, *CNS* central nervous system, *NE* not examined)

Day p.i.	2-μl inoculum ($n=5$)			20-μl inoculum ($n=5$)		
	Nose	Lungs	CNS	Nose	Lungs	CNS
2	5/5	0/5	0/3	5/5	5/5	0/3
3	5/5	0/5	3/3	5/5	5/5	3/3
4	5/5	3/5	3/3	5/5	5/5	3/3
5	5/5	4/5	3/3	5/5	5/5	3/3
7	1/1[a]	1/1[a]	1/1[a]	NE	NE	NE

[a]Only surviving mice were examined

2% non-fat dry milk in PBS and reacted with the antiserum. After washing in PBS-Tween 20, the filters were incubated with biotinylated goat anti-rabbit IgG, followed by streptavidin-alkaline phosphatase. The filters were developed in NBT/BCIP.

Histology and immunohistochemistry

The tissue obtained at autopsy was fixed in 4% formaldehyde prepared in PBS, and subsequently embedded in paraffin. For bony tissue, decalcification was achieved in EDTA solution before embedding. The maxillary region containing the nasal cavity was embedded in four portions after step-wise coronal sections. The lungs were transversely cut three times. The brain was cut four times at the frontal plane. Paraffin sections were analyzed by histological and immunohistochemical methods. Immunohistochemistry for detection of the viral antigen was performed by the avidin-streptavidin peroxidase method using diaminobenzidine as chromogen, as described previously [9, 15]. Topographical analysis was performed on 10-μm-step frontal or sagittal sections of whole mount-embedded brain tissue.

Results

Antibody characterization

We characterized the antigens of HK483 virus recognized by the anti-influenza A nucleoprotein antiserum prepared by immunizing rabbits with a purified nucleoprotein of influenza virus A H1N1 (PR8) [20]. In a Western blot analysis, this rabbit serum was shown to react with a 58-kDa band, consistent with the expected size of nucleoprotein in MDCK cells at 48 h after inoculation with HK483 virus. In addition, three minor bands of 110 (dimeric form), 48 and 43 kDa were recognized. A faintly stained band at 60 kDa was seen in uninfected cells (Fig. 1). Thus, this antibody was shown to principally recognize the HK483 virus.

Survival of mice after intranasal inoculation

We infected eight 4-week-old SPF ddY mice with 2 μl inoculum containing 1×10^5 PFU of HK483 virus into both nostrils. All of inoculated mice died within 8 days post inoculation (p.i.) (Fig. 2A). In contrast, the five control and five mice inoculated with 2 μl phosphate buffer or PR8 showed no fatal outcome.

Virus titers in the brain, lung and blood after intranasal inoculation

To investigate the viral dissemination in the mice inoculated with 2 μl virus suspension containing 2×10^5 PFU of HK483 virus, the virus amount in the lung and brain of three infected mice was determined on days 2, 3, 4, 5 and 6 p.i. In addition, viral titers in the blood were also examined on days 4 and 6 p.i. Virus was isolated from the brain and lungs from day 2 p.i. onwards, but first became measurable on day 3 p.i. in both tissues (Fig. 2B). Although the viral titers were higher in the lungs than in the brain, the virus replication in the lungs and in the brain rose in a similar pattern. Virus was also isolated from the blood but titers were less than one fifth of those in lungs and brain.

Distribution of virus-infected cells in the nasal cavity, lungs and brain

We analyzed the localization of the virus antigen-positive cells in the paraffin sections of tissue from three to five mice by an immunohistochemical method using anti-influenza virus A nucleoprotein antiserum. Initially, we confirmed that there was no cross-reaction of this antiserum with normal mouse tissues (without viral infection, data not shown). Mice were inoculated with 2 μl or 20 μl of virus solutions containing the same titer of HK483 virus and autopsied from days 2 to 7 p.i. On day 2 p.i. virus-infected cells were detected in the nasal cavity in mice infected with both 2 μl and 20 μl, but only in the lungs in mice inoculated with the 20-μl volume (Table 1). On day 3 p.i. infected cells were observed in the brains of mice inoculated with the different volumes; however, no antigen-positive cells were detected in the three transverse sections of the lungs of mice infected with a 2-μl inoculum. For these mice, virus-infected cells first appeared in the lungs from day 4 p.i. It therefore became apparent that CNS involvement was not correlated with viral infection in the lungs.

In the CNS of mice inoculated with a 2-μl volume, virus-infected cells were initially detected in the trigeminal nuclei and ganglia, and thereafter increased in number and foci. To clarify which cells were susceptible to this virus and the pathway of viral spread within the CNS, we examined the topographical localization of virus-infected cells in CNS by serial sectioning of the whole brain of mice inoculated with a 20-μl volume.

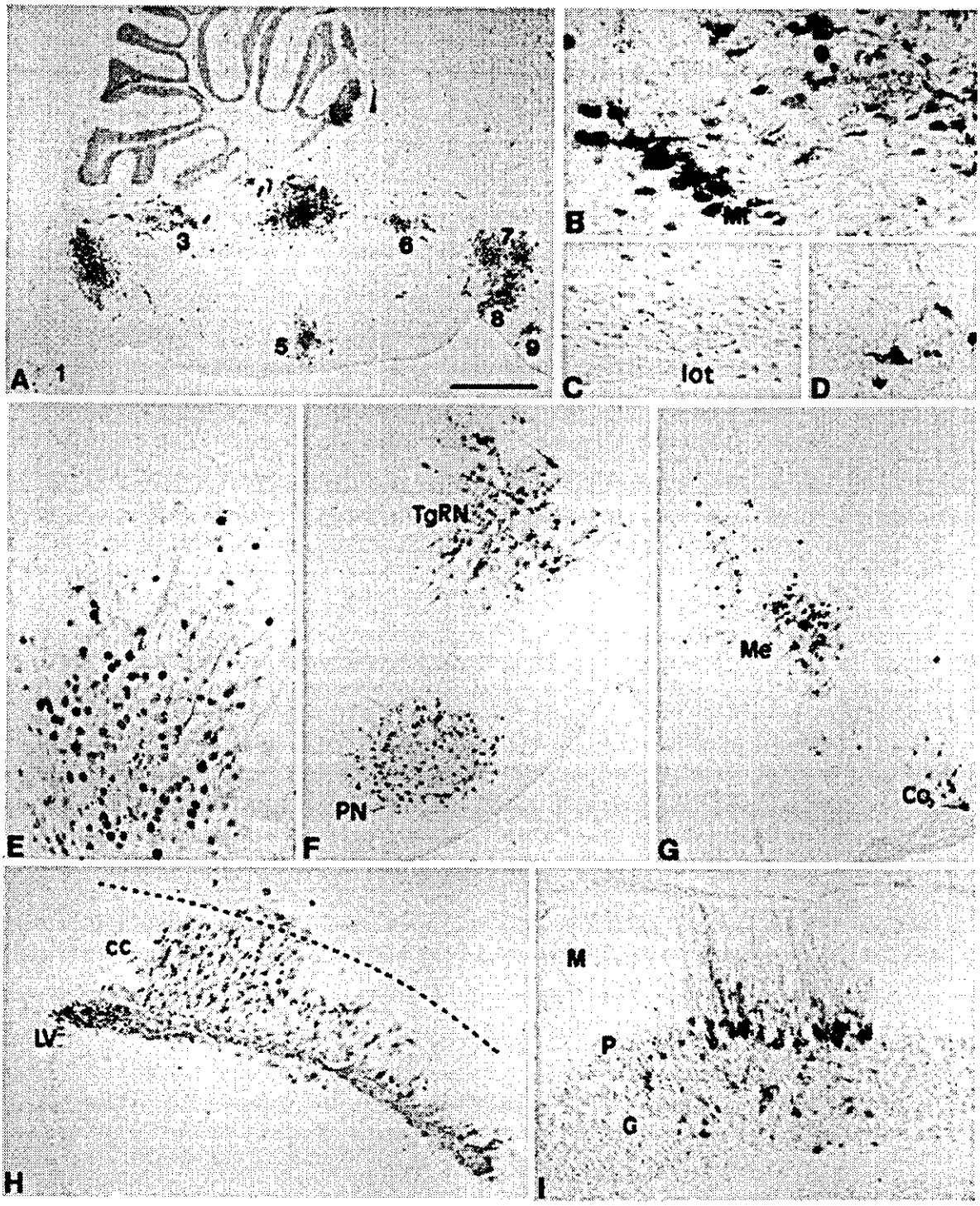

In the CNS, HK483 virus mainly infected neurons (Figs. 3A–I, 4A–C). Around these infected neurons, some glial cells were also positive for the viral antigens (Figs. 3B, D, E; 5A, B). In the center of lesion, both the nuclei and cytoplasm of neurons were frequently positive, whereas in their periphery only the nuclei were positive (Fig. 3E). Some ependymal cells were also infected (Fig. 3H). Viral infection was recognized in the cervical spinal cord, the caudal brain and rostral cerebellar folium on day 4 p.i., and was widespread on day 7 p.i. (Table 2). In the brainstem, the nuclei of nerves innervating the facial region (trigeminal and vestibular nuclei), pontine reticular formation, and substantia nigra were infected (Fig. 3A, F). In addition, the olfactory

◀

Fig. 3 Parasagittal section (rostral to the *right*) of a mouse intranasally inoculated with 20 µl of H5N1 virus on day 4 p.i. **A** Infected foci in the cervical spinal cord (*1*) and the caudal brain; the caudal spinal trigeminal nucleus (*2*), the nucleus of solitary tract (*3*), the medial vestibular nucleus (*4*), perifacial pontine reticular region (*5*), the rostral pontine reticular formation (*6*), the ventral tegmental area (*7*) and the substantia nigra (pars compacta, *8*; and pars reticulata, *9*). Rostral cerebellar folium is also infected. **B–G** Positive cells in the olfactory bulb (B) (*Mi* mitral cells), positive fibers in the lateral olfactory tract (**C**), positive cells in the olfactory tubercle (**D**), the visual cortex (**E**), the pontine tegmental reticular nucleus (*TgRN*), and the pontine nuclei proper (*PN*) (**F**), and the medial (*Me*) and cortical (*Co*) nuclei of the amygdaloid complex (**G**). **H** Positive ependymal cells of the lateral ventricle (*LV*), glial cells in the corpus callosum (*cc*), and deep cortical neurons. **I** Positive cells in the cerebellar cortex (*G* granular layer, *P* Purkinje cell layer, *M* molecular layer). Immunohistochemistry (peroxidase/diaminobenzidine) for the nucleoprotein of influenza A virus counterstained with methylgreen. *Bar* **A** 1 µm; **B–D** 50 µm; **E** 100 µm; **F–I** 200 µm

system (olfactory epithelium, olfactory bulb, lateral olfactory tract and olfactory tubercle) (Figs. 3B–G), visual (Fig. 3E) and cerebellar cortices (Fig. 3I), and ventricular ependymal cells (Fig. 3H) were involved. On 7 day p.i., viral infection became extensive and the virus-infected cells were disseminated in most of caudal brainstem and cerebellar nuclei, globus pallidus, and hypothalamic area (Fig. 4A–C).

The principal histological changes of the CNS were necrotic changes of neurons and glial and ependymal cells with granulocytic infiltration (Fig. 6). Some neurons showed karyorrhexis or pyknosis. Subarachnoid infiltration was focally observed but perivascular cuffing and glial nodules were not conspicuous. In the nasal cavity, virus infected the columnar and olfactory epithelial cells, and the subepithelial cells beneath the olfactory epithelium (Fig. 7) on day 3 p.i. Mice infected with the PR8 virus showed a localized infection of the respiratory tract without viral dissemination to the brain, spinal cord, heart or liver; only the epithelial cells were infected by PR8.

Discussion

Although no histological analysis of the brains of fatal human cases has been reported, animal models of H5N1 virus infection in mice and birds disclosed that it causes a generalized infection with marked neural involvement [15]. In this study, we have shown that nasal infection without marked pulmonary involvement is sufficient to cause CNS infection. Usual influenza A viruses, such as H1N1, H2N2, and H3N1, become infectious after cleavage of HA protein to HA_1 and HA_2 subunits by extracellular protease present in the respiratory lumen [10]. However, H5N1 virus is made infectious by intracellular protease [8], and may therefore spread in tissue without any extracellular proteases or with inhibitors to these proteases. This difference in HA proteins is important in viral invasiveness. H5N1 virus can infect

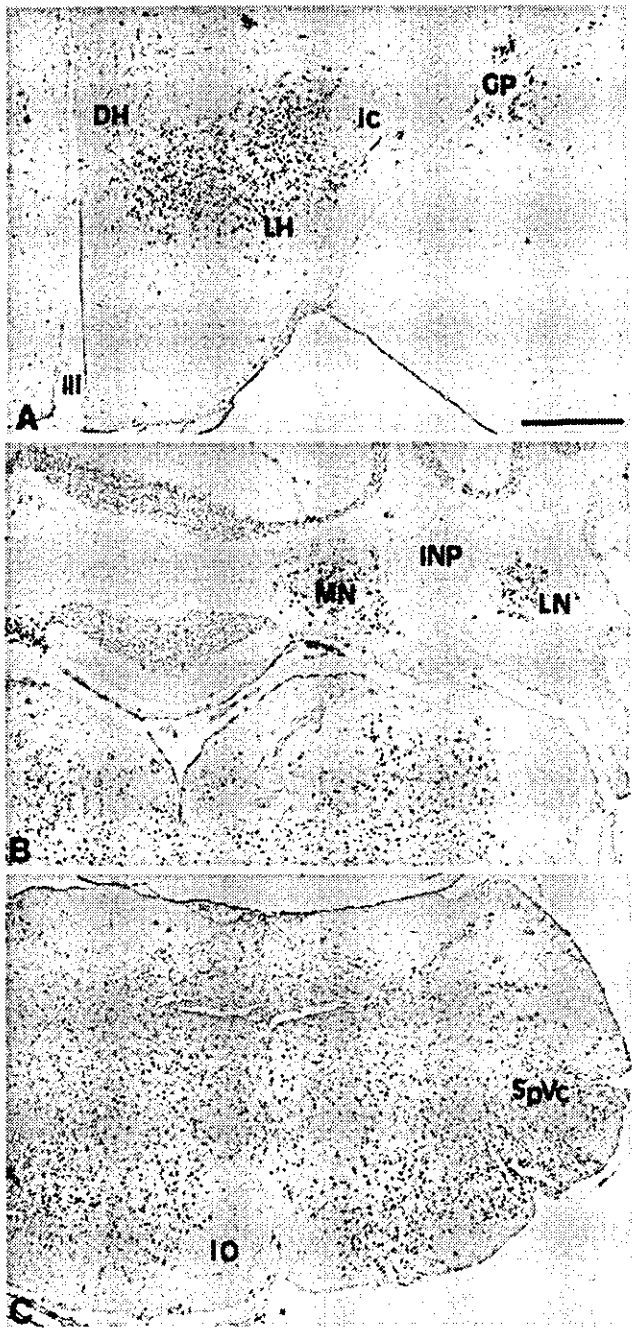

Fig. 4 Extensive viral spread in the central nervous system of a mouse inoculated with 20 µl inoculum on day 7 p.i. **A** The lateral hypothalamic area (*LH*), globus pallidus (GP), dorsomedial hypothalamus (*DH*), third ventricle (*III*). **B** Pons and the cerebellum: medial (*MN*) and lateral (*LN*) deep cerebellar nuclei (*INP* interposed nuclei). **C** The caudal brainstem: the caudolateral regions of inferior olive (*IO*) is intact (*SpVc* caudal spinal trigeminal nucleus). Immunohistochemistry (peroxidase/diaminobenzidine) for the nucleoprotein of influenza A virus counterstained with methylgreen. *Bar* **A–C** 500 µm

the subepithelial cells directly and spread in a cell to cell fashion, as observed in this study, but usual influenza A virus only infects the surface epithelium and never